Available at
www.ElsevierComputerScience.com
POWERED BY SCIENCE DIRECT®
Parallel Computing 29 (2003) 1381–1401

PARALLEL COMPUTING

www.elsevier.com/locate/parco

Data-parallel polygonization ☆

Erik G. Hoel [1], Hanan Samet *

Department of Computer Science, Institute of Advanced Computer Studies, Center for Automation Research, University of Maryland, College Park, MD 20742, USA

Received 2 April 2002; accepted 30 May 2003

Abstract

Data-parallel algorithms are presented for polygonizing a collection of line segments represented by a data-parallel bucket PMR quadtree, a data-parallel R-tree, and a data-parallel R^+-tree. Such an operation is useful in a geographic information system (GIS). A sample performance comparison of the three data-parallel structures for this operation is also given.

Keywords: Data-parallel algorithms; Polygonization; Hierarchical spatial data structures; Lines

1. Introduction

Spatial data consists of spatial objects made up of points, lines, regions, rectangles, surfaces, volumes, and even data of higher dimension which includes time. Examples of spatial data range from locations of cities, rivers, roads, to the areas that are spanned by counties, states, crop coverages, mountain ranges, etc. Such data is useful in applications in environmental monitoring, space, urban planning, resource management, and geographic information systems (GIS) [14,29].

There are many different representations of spatial data, the most prominent being the quadtree, R-tree, and R^+-tree (see [26,27] for an overview). There has not been much research on the use of such representations in a parallel environment.

☆ This work was supported in part by the National Science Foundation under grants EIA-99-00268, EAR-99-05844, IIS-00-86162, and EIA-00-91474 and Los Alamos Scientific Laboratory under Contract 6255U00153Q.

* Corresponding author. Tel.: +1-301-405-1755; fax: +1-301-314-9115.
E-mail address: hjs@umiacs.umd.edu (H. Samet).
[1] Present address: ESRI 380 New York Street Redlands, CA 92373-8100, USA.

0167-8191/$ - see front matter © 2003 Published by Elsevier B.V.
doi:10.1016/j.parco.2003.05.001

The most notable has been the work of Bestul [3] who considered a number of quadtree variants and showed how to construct them, as well as how to conduct a limited number of operations on data-parallel quadtrees for regions. His approach was conducted under the data-parallel SAM model of computation [3] which is a subset of the more general scan model [4]. The R-tree research has been limited to the development of algorithms for single cpu-multiple parallel disk systems [18], but no work has been performed on data-parallel R-trees or R^+-trees.

In this paper we examine the use of data-parallel versions of the quadtree, R-tree, and R^+-tree for the polygonization operation. Polygonization is the process of determining all closed polygons formed by a collection of planar line segments. We identify each polygon uniquely by the bordering line with the lexicographically minimum identifier (i.e., line number) and the side on which the polygon borders the line. Polygonization may be performed in a straightforward fashion without relying upon a data-parallel spatial data structure. In essence, the lines could be sorted based upon their identifier in $O(\log n)$ time. Next, each line, in sorted sequence, would transmit its endpoint coordinates, line identifier, and current left and right polygon identifiers to all following lines via a sequence of $O(n)$ scan operations. Each line would independently be able to determine the identifiers of the left and right polygons. The drawback of this approach is that it is an $O(n)$ operation with a large number of scans. By employing a data parallel spatial data structure, the number of global scan operations (i.e., a scan across the entire processor set) may be reduced by, instead, relying upon segmented scans executed in parallel (where each segment consists of a small number of lines) thereby speeding the computation.

The rest of this paper is organized as follows. Section 2 reviews sequential spatial data structures. Section 3 presents the data-parallel computation model while Section 4 reviews the polygonization process. Sections 5–7 describe how to perform polygonization for the bucket PMR quadtree, the R-tree, and the R^+-tree. Section 8 contains the results of a small performance study. Concluding remarks are drawn in Section 9.

2. Sequential spatial data structures

We are interested in representations that are based on spatial occupancy. Spatial occupancy methods decompose the space from which the data is drawn (e.g., the two-dimensional space containing the lines) into regions called *buckets*. They are also commonly known as *bucketing methods*. Traditionally, bucketing methods such as the grid file [23], BANG file [12], LSD trees [16], Buddy trees [31], BV-trees [11], PK trees [33], etc. have usually been applied to points. In contrast, we are applying the bucketing methods to the space from which the data is drawn (i.e., two-dimensions in the case of a collection of line segments which is the domain used in the rest of this paper).

There are four principal approaches to decomposing the space from which the data is drawn. One approach buckets the data based on the concept of a minimum bounding (or enclosing) rectangle. In this case, objects are grouped (hopefully by

proximity) into hierarchies, and then stored in another structure such as a B-tree [7]. The R-tree (e.g., [2,15]) is an example of this approach.

The R-tree and its variants are designed to organize a collection of arbitrary spatial objects (most notably two-dimensional rectangles) by representing them as d-dimensional rectangles. Each node in the tree corresponds to the smallest d-dimensional rectangle that encloses its son nodes. Leaf nodes contain pointers to the actual objects in the database, instead of sons. The objects are represented by the smallest aligned rectangle containing them.

The basic rules for the formation of an R-tree are very similar to those for a B-tree. All leaf nodes appear at the same level. Each entry in a leaf node is a 2-tuple of the form (R, O) such that R is the smallest rectangle that spatially contains object O. Each entry in a non-leaf node is a 2-tuple of the form (R, P) such that R is the smallest rectangle that spatially contains the rectangles in the child node pointed at by P. An R-tree of order (m, M) means that each node in the tree, with the exception of the root, contains between $m \leqslant \lceil M/2 \rceil$ and M entries. The root node has at least two entries unless it is a leaf node.

For example, consider the collection of line segments given in Fig. 1 shown embedded in a 4×4 grid. Let $M = 3$ and $m = 2$. One possible R-tree for this collection is given in Fig. 2a. Fig. 2b shows the spatial extent of the bounding rectangles of the nodes in Fig. 2a, with broken lines denoting the rectangles corresponding to the subtrees rooted at the non-leaf nodes. Note that the R-tree is not unique. Its structure depends heavily on the order in which the individual line segments were inserted into (and possibly deleted from) the tree.

The drawback of these methods is that they do not result in a disjoint decomposition of space. The problem is that an object is only associated with one bounding rectangle (e.g., line segment i in Fig. 2 is associated with rectangle $R5$, yet it passes through $R1$, $R2$, $R4$, and $R5$). In the worst case, this means that when we wish to determine which object is associated with a particular point (e.g., the containing rectangle in a rectangle database, or an intersecting line in a line segment database) in

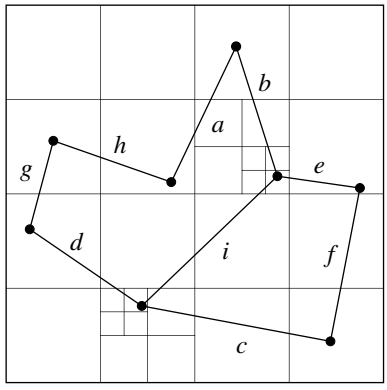

Fig. 1. Example collection of line segments embedded in a 4×4 grid.

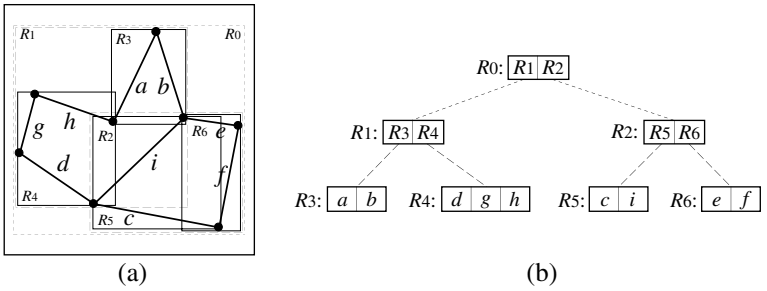

Fig. 2. (a) R-tree for the collection of line segments in Fig. 1, and (b) the spatial extents of the bounding rectangles.

the two-dimensional space from which the objects are drawn, we may have to search the entire database.

The other approaches are based on a decomposition of space into disjoint cells, which are mapped into buckets. Their common property is that the objects are decomposed into disjoint subobjects such that each of the subobjects is associated with a different cell. They differ in the degree of regularity imposed by their underlying decomposition rules and by the way in which the cells are aggregated. The price paid for the disjointness is that in order to determine the area covered by a particular object, we have to retrieve all the cells that it occupies.

The first method based on disjointness partitions the objects into arbitrary disjoint subobjects and then groups the subobjects in another structure such as a B-tree. The partition and the subsequent groupings are such that the bounding rectangles are disjoint at each level of the structure. The R^+-tree [32] and the cell tree [13] are examples of this approach. They differ in the data with which they deal. The R^+-tree deals with collections of objects that are bounded by rectangles, while the cell tree deals with convex polyhedra.

The R^+-tree is an extension of the k-d-B-tree [25]. The R^+-tree is motivated by a desire to avoid overlap among the bounding rectangles. Each object is associated with all the bounding rectangles that it intersects. All bounding rectangles in the tree (with the exception of the bounding rectangles for the objects at the leaf nodes) are non-overlapping. [2] The result is that there may be several paths starting at the root to the same object. This may lead to an increase in the height of the tree. However, retrieval time is sped up.

Fig. 3 is an example of one possible R^+-tree for the collection of line segments in Fig. 1. This particular tree is of order $(2, 3)$ although in general it is not possible to guarantee that all nodes will always have a minimum of two entries. In particular, the expected B-tree performance guarantees are not valid (i.e., pages are not guaranteed to be m/M full) unless we are willing to perform very complicated record inser-

[2] From a theoretical viewpoint, the bounding rectangles for the objects at the leaf nodes should also be disjoint. However, this may be impossible (e.g., when the objects are line segments where many line segments intersect at a point).

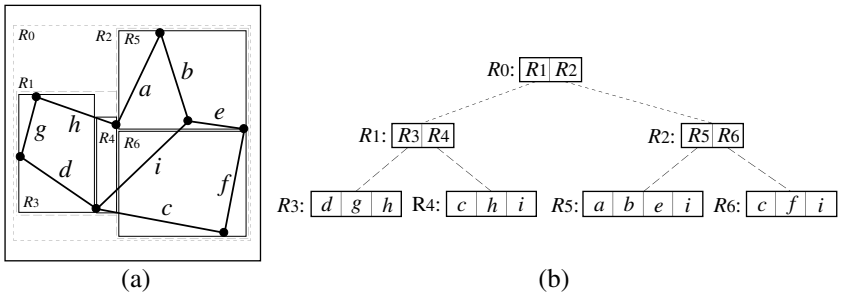

Fig. 3. (a) R^+-tree for the collection of line segments in Fig. 1 and (b) the spatial extents of the bounding rectangles.

tion and deletion procedures. Notice that line segments *c* and *h* appear in two different nodes, while line segment *i* appears in three different nodes. Ofcourse, other variants are possible since the R^+-tree is not unique.

Methods such as the R^+-tree and the cell tree (as well as the R*-tree [2]) have the drawback that the decomposition is data-dependent. This means that it is difficult to perform tasks that require composition of different operations and data sets (e.g., set-theoretic operations such as overlay). In contrast, the remaining two methods, while also yielding a disjoint decomposition, have a greater degree of data-independence. They are based on a regular decomposition. The space can be decomposed either into blocks of uniform size (e.g., the uniform grid [10]) or adapt the decomposition to the distribution of the data (e.g., a quadtree-based approach such as [28]). In the former case, all the blocks are of the same size (e.g., the 4×4 grid in Fig. 1). In the latter case, the widths of the blocks are restricted to be powers of two, and their positions are also restricted.

There are a number quadtree-based approaches [27] for storing collections of line segments. They differ by being either vertex-based [28] or edge-based [21,22]. Their implementations make use of the same basic data structure. All are built by applying the same principle of repeatedly breaking up the collection of vertices and edges (making up the collection) into groups of four blocks of equal size (termed *brothers*) until obtaining a subset that is sufficiently simple so that it can be organized by some other data structure. This is achieved by successively weakening the definition of what constitutes a legal block, thereby enabling more information to be stored in each bucket.

The bucket PMR quadtree [19] is an example of an edge-based quadtree representation. Each block (or bucket) is split repeatedly until each sub-block contains no more than *b* lines, where *b* is the bucket capacity. For example, Fig. 4 shows the block decomposition corresponding to the bucket PMR quadtree for the collection of line segments in Fig. 1 with a bucket capacity 2 and maximal tree height 3. We do not show the tree representation. There are a total of 10 blocks or buckets with three of the blocks or buckets being empty. Note that unless the bucket capacity is greater than or equal to the maximal number of possible intersections, the recursive decomposition will continue to the maximal depth allowed by the bucket PMR quadtree (e.g., the endpoints of line segment *i* in Fig. 4 subdivide until reaching depth 3).

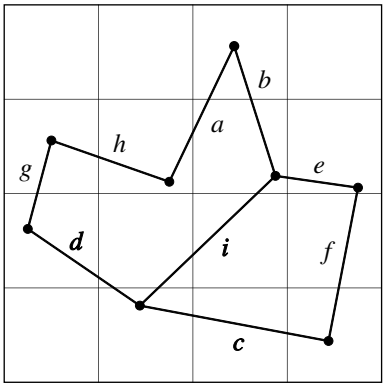

Fig. 4. The block decomposition corresponding to the bucket PMR quadtree for the collection of line segments in Fig. 1.

The uniform grid is ideal for uniformly distributed data, while quadtree-based approaches are suited for arbitrarily distributed data. In the case of uniformly distributed data, quadtree-based approaches degenerate to a uniform grid, albeit they have a higher overhead. Both the uniform grid and the quadtree-based approaches lend themselves to set-theoretic operations. Thus they are ideal for tasks which require the composition of different operations and data sets. In general, since spatial data is not usually uniformly distributed, the quadtree-based regular decomposition approach is more flexible.

3. Data-parallel computation model

We make use of the scan model [6] which is a general-purpose model of parallel computation defined in terms of a collection of primitive operations that can operate on arbitrarily long vectors (single dimensional arrays) of data. Three types of primitives (scan, elementwise, and permutation) are used to produce result vectors of equal length. A *scan* primitive is an operation [30] (or parallel prefix operation) that takes an associative operator $\oplus$, an input vector $[a_0, a_1, \ldots, a_{n-1}]$, and returns the result vector $[a_0, (a_0 \oplus a_1), \ldots, (a_0 \oplus a_1 \oplus \cdots \oplus a_{n-1})]$.

The scan model is an EREW PRAM [17] that includes the scan operations as primitives [5]. The scan model considers all primitive operations (including scans) as taking unit time [3] on a hypercube architecture. This allows sorting operations

[3] Blelloch [5] points out that algorithmic models, which supply a simple abstraction of a computing device, specify a set of primitive operations that are assumed to execute in "unit time". The unit time assumption aids the researcher in analyzing algorithms. However, the unit time operations may often take time which is dependent upon the machine and algorithm parameters. Additionally, some scan operations can execute in less cpu time than parallel memory references. It has been confirmed that this is approximately the case for integer scan operations [8].

to be performed in $O(\log n)$ time using a simple radix sort. Despite being a general-purpose model of parallel computation, the scan model has been efficiently implemented on massively parallel processors such as the Thinking Machines CM-2 and CM-5.

Scan operations may be classified in a number of ways. Given a linear ordering of n processors $[a_0, a_1, \ldots, a_{n-1}]$, a scan may be classified as either *upward* or *downward*. An upward scan (also termed a *forward scan* or a *parallel prefix* operation), returns the vector $[a_0, (a_0 \oplus a_1), \ldots, (a_0 \oplus a_1 \oplus \cdots \oplus a_{n-1})]$. In essence, the ith processor in the linear ordering receives the result of applying an associative operator to the values of the preceding $i-1$ processors. Analogously, a downward scan (also termed a *backward scan* or a *parallel suffix* operation), returns the vector $[(a_0 \oplus a_1 \oplus \cdots \oplus a_{n-1}), (a_1 \oplus a_2 \oplus \cdots \oplus a_{n-1}), \ldots, a_{n-1}]$.

In addition to being classified as either upward or downward, scan operations may be *segmented* or *unsegmented*. An unsegmented scan is a simple scan across all processors in the linear ordering. A segmented scan, however, may be thought of as multiple parallel scans, where each scan operates independently on a segment of contiguous processors. The segmented groups of processors in the linear ordering (or *segment groups*) are commonly delimited by a *segment flag*, where a value of 1 denotes the first processor in the segment.

Finally, scan operations may be classified as being either *inclusive* or *exclusive*. For example, an upward *inclusive* scan operation returns the result vector $[a_0, (a_0 \oplus a_1), \ldots, (a_0 \oplus a_1 \oplus \cdots \oplus a_{n-1})]$, while an upward *exclusive* scan returns the vector $[0, a_0, \ldots, (a_0 \oplus a_1 \oplus \cdots \oplus a_{n-2})]$.

An *elementwise* primitive is an operation that takes two vectors of equal length and produces an answer vector, also of equal length. The ith element in the answer vector is the result of the application of an arithmetic or logical primitive to the ith elements of the input vectors. A *permutation* primitive takes two vectors, the data vector and an index vector, and rearranges (permutes) each element of the data vector to the position specified by the index vector. Note that the permutation must be one-to-one; two or more data elements may not share the same index vector value.

The SAM (scan-and-monotonic-mapping) model [3] is a similar but more restrictive model of parallel computation. It makes use of one or more linearly ordered sets of processors which allow elementwise and scanwise operations to be performed. In addition, both within and between each linearly ordered set of processors, *monotonic mappings* may be performed. A monotonic mapping is defined as one in which the destination processor indices are a monotonically increasing or monotonically decreasing function of the source processor indices. Thus arbitrary permutations are not allowed in the SAM model. The SAM model affords more efficient hypercube routing than the standard scan model, thus providing motivation for the more restrictive model [3].

The SAM model was useful for the bucket PMR quadtree for which, because of its regular disjoint decomposition, a unique linear ordering may readily be obtained (given a particular linear ordering methodology such as a Peano curve [24]). However, the R-tree and the R^+-tree, because of their irregular decomposition, do not have a unique linear ordering thereby necessitating expensive processor reorderings

if we wish to maintain monotonic mappings between their leaf nodes. Thus we adhere to the scan model in the rest of this paper.

4. Polygonization

The goal of the polygonization process is to label each line segment with two unique identifiers: one for the polygon on its left and one for the polygon on its right. The polygons are represented by a partial winged-edge representation [1]. The winged-edge representation enables us to determine all edges that comprise a polygon in time proportional to the number of edges in the polygon, and all edges that meet at a vertex in time proportional to the number of edges that are incident at the vertex. We illustrate our discussion with the aid of Fig. 5. Each line segment z in the collection is assumed to be directed which means that z has a source and destination vertex. The partial winged-edge representation contains an association between the incident line segments at each of the endpoints of z. In particular, there are two polygons associated with each side of z: one on the left and one on the right, where left and right are with respect to the direction of z. For example, for the polygon on the left of z, the incoming edge (i.e., at the source vertex) is the one at the minimal angle formed by the edges incident at the source vertex and z. Similarly, the outgoing edge (i.e., at the destination vertex) is the one at the maximal angle formed by the edges incident at the destination vertex and z. On the other hand, for the polygon on the right of z, the incoming edge (i.e., at the source vertex) is the one at the maximal angle formed by the edges incident at the source vertex and z. Similarly, the outgoing edge (i.e., at the destination vertex) is the one at the minimal angle formed by the edges incident at the destination vertex and z.

Using Fig. 5 as an example, the left polygon identifier for line segment z is selected from the minimum identifiers (assuming a lexicographic ordering) of the source endpoint minimal angle (w_R, where w is the line identifier and R denotes the right side of w), the destination endpoint maximal angle (y_R), and the line identifier itself (z_L). For the right polygon identifier, select the minimum identifier among the source endpoint maximum angle (x_R), the destination endpoint minimal angle (v_R), and the line identifier (z_R). Therefore, in Fig. 5, line z is assigned w_R as the initial left polygon identifier, and v_R as the right polygon identifier.

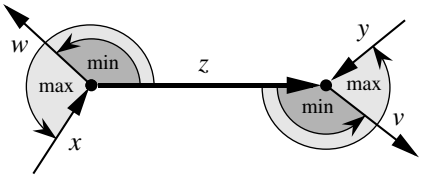

Fig. 5. Selecting the initial polygon identifiers.

5. Polygonization using the bucket PMR quadtree

The data-parallel PMR quadtree is formed in the same way as the sequential variants. Given a bucket PMR quadtree, the polygonization process begins by constructing a partial winged-edge representation as described in Section 4. In constructing the partial winged-edge representation, the endpoints of each line in a node are broadcast to all other lines in the node through a series of segmented scans. By *broadcast* we mean the process of transmitting a constant value from a single processor to all other processors in the same segment group via a scan operation (i.e., the vector $[a_0, a_0, \ldots, a_0]$). This iterative process is bounded by the maximal number of lines contained in any node within the quadtree. In most cases, this will equal the bucket capacity of the quadtree. Locally, each line processor maintains the minimal and maximal angles formed at each endpoint as well as the identities of the corresponding lines. Once the broadcasts are completed, each line processor locally assigns an initial polygon identifier to the bordering polygon on the left and right side (moving from source to destination endpoint).

Next, nodes are merged and duplicate line segments are eliminated. As the duplicated line segments are eliminated, we update the polygon identifiers that are associated with their sides to the minimum of the identifiers that are currently associated with them. For example, if two instances of line z are merged so that the polygon identifiers associated with the left and right sides of the first instance are a_L and d_R, respectively, and the polygon identifiers associated with the left and right sides of the second instance are b_L and c_R, respectively, then, assuming a lexicographic minimum, the result is that a_L and c_R are the polygon identifiers that are now associated with the left and right sides of the surviving instance of z. In addition, the update step ensures that all instances of b_L and d_R are replaced by a_L and c_R, respectively.

We now show how the polygonization process works for the bucket PMR quadtree corresponding to the collection of line segments given in Fig. 1. Fig. 6 shows the initial polygon assignment for the depicted example where the left and right polygon identifiers are contained in the L_{ID} and R_{ID} fields, respectively. The nodes on the left side of the figure are labeled with numbers corresponding to the order in which they would be visited by a traversal of the corresponding quadtree in the recursive `NW`, `NE`, `SW`, and `SE` order. For each node n in the left side of the figure, we show a pair of

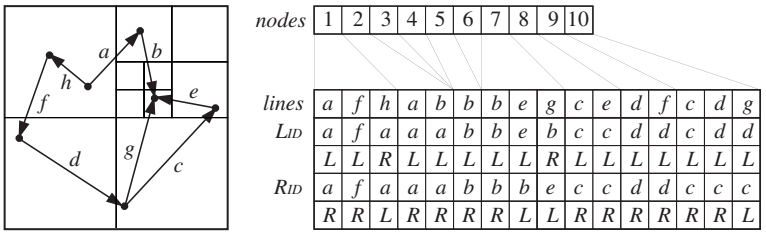

Fig. 6. Initial polygon assignments.

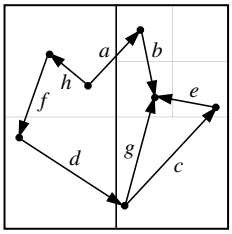

nodes	1	2	3	4	5	6	7									
lines	*a*	*f*	*h*	*a*	*b*	*b*	*b*	*e*	*g*	*c*	*e*	*d*	*f*	*c*	*d*	*g*
LID	*a*	*f*	*a*	*a*	*a*	*b*	*b*	*e*	*b*	*c*	*c*	*d*	*d*	*c*	*d*	*d*
	L	*L*	*R*	*L*	*L*	*L*	*L*	*L*	*R*	*L*	*L*	*L*	*L*	*L*	*L*	*L*
RID	*a*	*f*	*a*	*a*	*a*	*b*	*b*	*b*	*e*	*c*	*c*	*d*	*d*	*c*	*c*	*c*
	R	*R*	*L*	*R*	*R*	*R*	*R*	*L*	*L*	*R*	*R*	*R*	*R*	*R*	*R*	*L*

Fig. 7. Result after merging and prior to duplicate deletion.

lines demarcating the set of line segments associated with n. For example, lines a, f, and h are associated with node 1, while line segments a and b are associated with node 2. On the other hand, no line segments are associated with nodes 3, 4, and 6.

Starting at the leaf level, sibling nodes are merged together into their parent nodes. For example, in Fig. 6, leaf nodes 4–7 are merged together, resulting in leaf node 4 in Fig. 7. All the lines in the merged sibling leaf nodes are sorted, and any duplicate lines are marked. In Fig. 6, the merging of sibling leaf nodes 4–7 will result in one pair of duplicate lines (line b) as there is a line b in nodes 5 and 7. The duplicate occurrences of line b are highlighted in Fig. 7 which shows the results of merging nodes 4–7 prior to duplicate deletion. Duplicate deletion (also known as *concentrate* [20]) is accomplished using an upward exclusive scan operation, followed by an elementwise subtraction, and finally by a permutation operation.

At this point, let us explain the parallel implementation of merging in more detail. First perform an elementwise operation to tag those nodes that must merge (based upon tree height). This is followed by a broadcast from the tagged merging nodes to their corresponding lines telling them they will be merging. Third, perform an upward scan (exclusive, addition) and a permutation to delete the merged nodes (4 sibling nodes become 1 node). Fourth, execute a broadcast operation from nodes to lines establishing where the node is now located in the linear ordering. Fifth, sort (via a permutation) the merging lines based upon their line identifiers. Sixth, perform an elementwise operation to tag the duplicate lines in a node. Seventh, for each set of duplicate line identifiers (in one merged node), two upward scans (inclusive, segmented) are made to update the left and right polygon identifier sets. Eighth, delete the duplicate lines. Ninth, do a broadcast from the first line in each segment group to its associated quadtree node.

In order to ensure that each duplicate line has consistent polygon identifiers as well as correct winged-edge representations, each duplicate line has its endpoints and polygon identifiers broadcast to the other duplicate lines in the merged node. If any of the polygon identifiers of the duplicates are updated, then the identifier updates must also then be broadcast among all other lines in the merged nodes. By *update*, we mean assigning a lexicographically smaller polygon identifier. For instance, in Fig. 8 the merging of sibling leaf nodes 2–5 will result in two pairs of duplicate lines (lines b and e) as shown in Fig. 9. For the duplicate occurrence of line b in the merged node, initially one instance has left and right polygon identifiers a_L

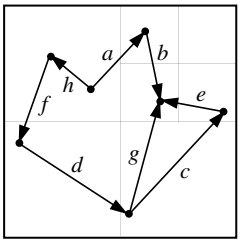

nodes	1	2	3	4	5	6	7							
lines	a	f	h	a	b	b	e	g	c	e	d	f	c	d	g
LID	a	f	a	a	a	b	e	b	c	c	d	d	c	d	d
	L	L	R	L	L	L	L	R	L	L	L	L	L	L	L
RID	a	f	a	a	a	b	b	e	c	c	d	d	c	c	c
	R	R	L	R	R	R	L	L	R	R	R	R	R	R	R

Fig. 8. Polygon assignments after the first iteration.

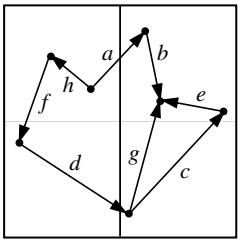

nodes	1	2	3	4											
lines	a	f	h	a	b	b	c	e	e	g	d	f	c	d	g
LID	a	f	a	a	a	b	c	e	c	b	d	d	c	d	d
	L	L	R	L	L	L	L	L	L	R	L	L	L	L	L
RID	a	f	a	a	a	b	c	b	c	e	d	d	c	c	c
	R	R	L	R	R	R	R	L	R	L	R	R	R	R	R

Fig. 9. Second round of merging prior to duplicate deletion. Duplicate lines b and e in node 2 are shaded.

and a_R, respectively, while the second instance has left and right polygon identifiers b_L and b_R, respectively. The left and right polygon identifiers of the second instance of line b are updated from b_L to a_L, and b_R to a_R, respectively.

If any line has its polygon identifiers updated during the first round of rebroadcasting, then the polygon identifier update must be communicated in a second round of broadcasting to all other lines in the merged node. Locally, if the transmitted polygon update matches either the left or right polygon identifiers of the local line, then the local polygon identifier is updated to reflect the polygon identifiers that have been broadcast.

For example, consider the situation depicted in Fig. 10 which is taken from the merging nodes shown in Fig. 9. The duplicate occurrences of line b result in two polygon updates (i.e., b_L to a_L and b_R to a_R) being broadcast to the other lines in

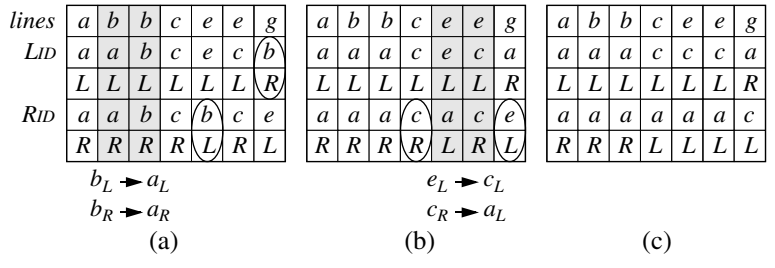

Fig. 10. Updating duplicate line b's polygon identifier.

the segment group. The other lines whose left or right polygon identifiers are then updated are shown as circled items in Fig. 10a. Specifically, these are the right polygon identifier of the first occurrence of line e, and the left polygon identifier of line g in the figure. Additionally, the two occurrences of line e also result in two broadcasted polygon updates (e_L to c_L and c_R to a_L) in Fig. 10b. The final result of the broadcasting of polygon identifiers necessitated by the duplicate occurrence of lines b and e is shown in Fig. 10c.

When the second instance of line b is updated, the two identifier updates are then broadcast to all other lines in the merged node. For each other line in the merged node, if the transmitted polygon identifier update matches either of its current left or right polygon identifiers, then the line's polygon identifier is changed to a_L in order to reflect the broadcast update and the lexicographically smaller identifier. In the example, the b_L to a_L update matches any line whose left or right polygon identifier have the value b_L. Similarly, the two occurrences of line e result in two additional identifier updates—that is, c_R to b_L, and e_L to c_L. Actually, line e's b_L was previously updated to a_L during the update broadcasts for line b.

Finally, when merging four sibling nodes together, any line whose endpoint falls on the shared node border (e.g., lines a and b in Fig. 11a), must also have its endpoints and polygon identifiers broadcast among the merged nodes. for example, consider Fig. 11a where four sibling nodes labeled A–D are being merged. For the sake of clarity, the contents of nodes C and D are not shown. There are no duplicate lines in the merging nodes, but lines a and b have an endpoint that intersects the common node border. The endpoint coordinates and polygon identifiers of these two lines are broadcast among the merged lines, and any appropriate winged-edge updates are made. In the figure, the source endpoint of line b is updated to reflect the incidence of line a. For all lines whose winged-edge representations are updated, the polygon identifiers are checked for possible updates. Fig. 11b shows the resulting polygon identifiers.

The merging and updating process continues up the entire bucket PMR quadtree until all lines are contained in a single node and all necessary broadcasts have been made. Fig. 12 depicts the polygon assignments after the second round of leaf node merging. Fig. 13 shows the result of the final round of merging, prior to duplicate deletion. In this figure, duplicate lines a, c, d, f, and g are shaded. In this case, line c's c_R is updated to a_L; line d's d_R and c_R to a_L; line f's f_R and d_R to a_L; line f's f_L and

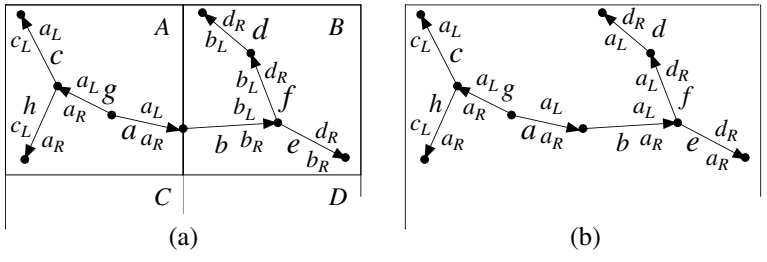

Fig. 11. Example of merging two leaf nodes.

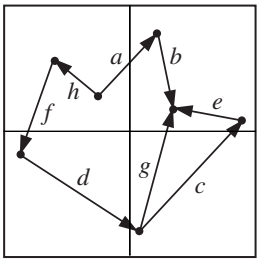

nodes	1	2	3	4									
lines	*a*	*f*	*h*	*a*	*b*	*c*	*e*	*g*	*d*	*f*	*c*	*d*	*g*
L_{ID}	*a*	*f*	*a*	*a*	*a*	*c*	*c*	*a*	*d*	*d*	*c*	*d*	*d*
	L	*L*	*R*	*L*	*L*	*L*	*L*	*R*	*L*	*L*	*L*	*L*	*L*
R_{ID}	*a*	*f*	*a*	*a*	*a*	*a*	*a*	*c*	*d*	*d*	*c*	*c*	*c*
	R	*R*	*L*	*R*	*R*	*L*	*L*	*L*	*R*	*R*	*R*	*R*	*L*

Fig. 12. Polygon assignments after the second round of merging.

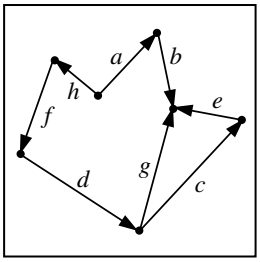

nodes	1											
lines	*a*	*a*	*b*	*c*	*c*	*d*	*d*	*e*	*f*	*f*	*g*	*g*	*h*
L_{ID}	*a*	*a*	*a*	*c*	*c*	*d*	*d*	*c*	*f*	*d*	*a*	*d*	*a*
	L	*L*	*L*	*L*	*L*	*L*	*L*	*L*	*L*	*L*	*R*	*L*	*R*
R_{ID}	*a*	*a*	*a*	*a*	*c*	*d*	*c*	*a*	*f*	*d*	*c*	*c*	*a*
	R	*R*	*R*	*L*	*R*	*R*	*R*	*L*	*R*	*R*	*L*	*L*	*L*

Fig. 13. Final round of merging, prior to duplicate deletion. Duplicate lines *a*, *c*, *d*, *f*, and *g* are shaded.

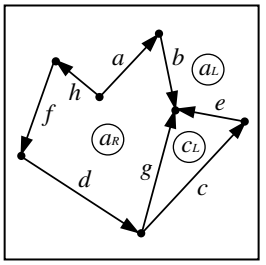

nodes	1							
lines	*a*	*b*	*c*	*d*	*e*	*f*	*g*	*h*
L_{ID}	*a*	*a*	*c*	*a*	*c*	*a*	*a*	*a*
	L	*L*	*L*	*R*	*L*	*R*	*R*	*R*
R_{ID}	*a*	*a*	*a*	*a*	*a*	*a*	*c*	*a*
	R	*R*	*L*	*L*	*L*	*L*	*L*	*L*

Fig. 14. Completion of the polygonization operation.

d_L to a_R; and line *g*'s d_L and c_L to a_R and a_L, respectively. Finally, Fig. 14 depicts the completion of the polygonization operation, with the final assigned polygon identifiers circled.

The bucket PMR quadtree's spatial sort greatly limits the amount of inter-segment communication necessary as compared with a non-spatially sorted dataset where all lines would have to communicate their endpoints and polygon identifiers to all others. In the worse-case, the bucket PMR quadtree polygonization algorithm has time complexity $O(n \log s)$, where n is the number of lines in the map that corresponds to a $s \times s$ image. However, this is usually not the case as the maximum number of lines in a segment is really the determinative cost factor and this number is usually considerably smaller than n. In particular, at each of the $O(\log s)$ stages of

the merging process, the number of scans is proportional to the number of lines intersecting the shared borders of the merging siblings. In the worse-case, all n lines are active at the final round of merging.

6. Polygonization using the R-tree

The data-parallel R-tree is formed in a different way than the sequential variant. The difference is that instead of inserting the line segments one-by-one into the data structure, all line segments are inserted simultaneously. There are a number of ways of determining the split with differing complexity. The goal is usually one of minimizing the overlap among the resulting nodes while retaining a certain minimal occupancy level. We do not discuss these issues further here.

The polygonization process for the data-parallel R-tree is similar to that described for the bucket PMR quadtree in Section 5. Given a data-parallel R-tree, we start by constructing a partial winged-edge representation. Once the partial winged-edge representation is completed, each line processor locally assigns an initial polygon identifier for the bordering polygon on the left and right side (see Section 5 for details).

The initial polygon assignment is shown in Fig. 15 for our example dataset where the left and right polygon identifiers are contained in processor sets L_{ID} and R_{ID}, respectively. Next, beginning with the nodes at the leaf level of the R-tree, we merge all sibling lines together into the parent nodes. All lines that intersect any of the overlapping regions formed by the bounding boxes of the nodes that have been merged are marked for rebroadcasting among the lines in the merged nodes. This is necessary in order to propagate the equivalence between the different identifiers in the merged nodes which represent the same polygon. We do not discuss the merging process further here.

For example, consider Fig. 16a where we have two R-tree nodes A and B that are to be merged. In this example, node A contains lines (a, c, g, h), and node B contains

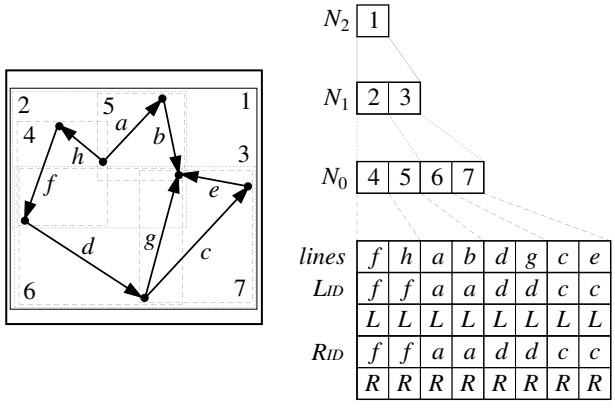

Fig. 15. Initial polygon assignments.

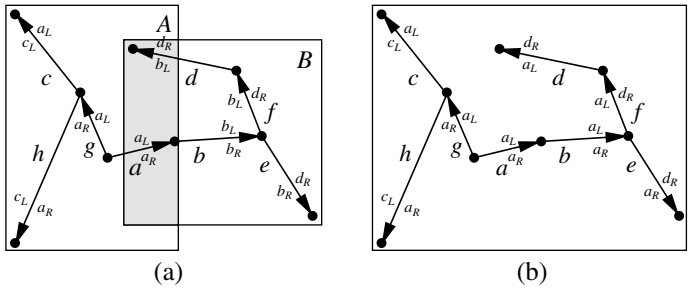

Fig. 16. Two R-tree nodes merging during polygonization.

lines (b, d, e, f). In the figure, lines (a, b, d) must be rebroadcast to the merged set of lines (a, b, c, d, e, f, g, h) as they intersect the overlapping region formed by the bounding boxes of nodes A and B. The purpose of this operation is to update the winged-edge representations of any necessary lines. In Fig. 16a, lines a and b require updating to take place. When the winged-edge representation is updated, we note any polygon identifiers that must also be updated. In the example in Fig. 16, line b has both its left and right polygon identifiers updated; b_L in Fig. 16a becomes a_L in Fig. 16b, and similarly, b_R becomes a_R. Line a does not have either of its polygon identifiers updated because its left and right polygon identifiers are lexicographically minimal.

For all such polygon identifier updates (e.g., b_L to a_L and b_R to a_R in Fig. 16), we broadcast the updates to all other lines in the merged node via scan operations. Locally, if the transmitted polygon update matches either the left or right polygon identifiers of the local line, then the local polygon identifier is updated to reflect the polygon identifiers that have been broadcast. For example, in Fig. 16a, the right polygon identifier of line e is updated to reflect the fact that polygon identifier b_R becomes a_R. Similarly, the left side polygon identifiers of lines d and f are updated to reflect the fact that polygon identifier b_L becomes a_L. The resulting polygon identifiers and merged nodes are depicted in Fig. 16b. The status of the R-tree polygonization operation for Fig. 15 after the first round of leaf node merging is shown in Fig. 17. This process continues up the entire R-tree until all lines are contained in a single node and all necessary broadcasts have been completed. The final configuration of our original example dataset is depicted in Fig. 18. Fig. 18 results from merging nodes 2 and 3 in Fig. 17, and performing the polygon identifier updates. In particular, the intersection of b and e leads to c_R being replaced by a_L, the intersection of b and g leads to d_L being replaced by a_R, and the intersection of d and f leads to d_R being replaced by a_L. The identifiers assigned to the three polygons are shown in the figure by enclosing the identifiers within circles.

The R-tree's spatial sort greatly limits the amount of inter-segment communication necessary as compared with a non-spatially sorted dataset where all lines would have to communicate their endpoints and polygon identifiers to all others. However, the non-disjoint decomposition of the R-tree causes increased computational complexities in the local broadcasting phase of the sibling merge operation

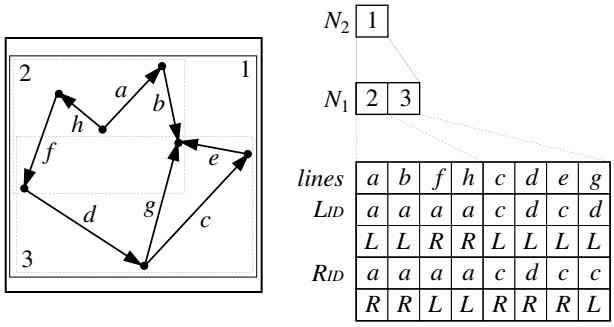

Fig. 17. Polygonization after first round of leaf node merging.

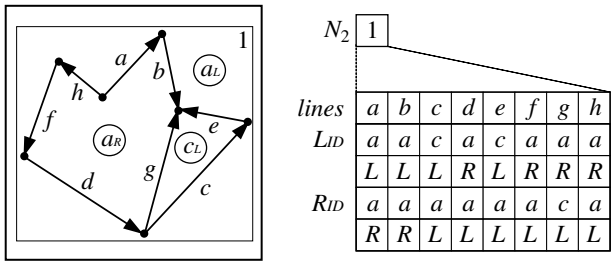

Fig. 18. Completion of the polygonization operation.

in comparison to an analogous disjoint decomposition spatial data structure such as the bucket PMR quadtree or the R^+-tree (see Section 7). This is because it is often the case that many lines fall in the intersecting areas when the R-tree nodes are merged. With representations based on a disjoint decomposition of space, only those lines that intersect the decomposition lines would need to be locally broadcast during the sibling merge operation.

Now, let us estimate the number of broadcasts necessary during the polygon identification process due to the lines intersecting overlapping regions. In the average-case, assume that each R-tree node has a fan-out of M. Let c (where $0 \leqslant c \leqslant 1$) be the fraction of the lines in each node that intersect one or more of the overlapping regions formed by the bounding boxes of the nodes that have been merged. Also, let h denote the height of the R-tree; without loss of generality, $h = \log_M n$, where n is the number of lines in the tree. Using the fact that $M^h = n$, it can be shown that the number of local broadcasts b that must be made during the merging phases due to the intersection of lines with the overlapping regions is

$$b = \sum_{i=2}^{h} cM^i \leqslant n\left(\frac{M}{M-1}\right).$$

This is in the worst-case $O(n)$. However, the average-case complexity is expected to be lower. In particular, the average-case complexity of the line broadcasting step is

dependent upon the ability of the node splitting algorithm to partition the buckets as much as possible (therefore lowering the fraction c of lines intersecting the overlapping regions).

7. Polygonization using the R^+-tree

As in the case of the R-tree, the data-parallel R^+-tree is formed in a different way than the sequential variant. Again, the difference is that instead of inserting the line segments one-by-one into the data structure, all line segments are inserted simultaneously with splits being made in accordance with the disjointness requirements as well as a minimal occupancy level. We do not discuss these issues further here.

The R^+-tree polygonization algorithm is very similar to that for the R-tree as described in Section 6. Because the R^+-tree employs a disjoint decomposition, a single line may reside in more than one leaf node, similar to the bucket PMR quadtree. In order to handle this difference with respect to the R-tree, the polygonization algorithm must be changed somewhat during the node-merging phase.

Instead of marking all lines that intersect any of the overlapping regions formed by the bounding boxes of the nodes that are being merged (as there are none with a disjoint decomposition), the update procedure follows the technique described for the bucket PMR quadtree polygonization algorithm in Section 5. All the lines in the merged sibling node are first sorted according to identifier, and all duplicate lines are marked for rebroadcasting among the lines in the merged nodes. This enables the correct updating of duplicate lines in the merged nodes. The duplicate node rebroadcasting operation is used to update the winged-edge representations of all duplicate lines and maintain consistency. During the update, we note any polygon identifiers that must also be updated. Among duplicate lines, if one line has polygon identifiers that are less than the polygon identifiers of the second line, then this inconsistency must be resolved, with the smaller identifier taking precedence over the larger. In addition, all lines whose endpoint falls on a common node border are marked for the rebroadcast of their endpoint coordinates in order to update the winged-edge representations and polygon identifiers of any line that may share an endpoint but lie in another node.

If any line has its polygon identifiers updated during the first round of rebroadcasting, then the polygon identifier update must be communicated in a second round of broadcasting to all other lines in the merged node. Locally, if the transmitted polygon update matches either the left or right polygon identifiers of the local line, then the local polygon identifier is updated to reflect the polygon identifiers that have been broadcast. This operation was described in Section 5.

As is the case for the bucket PMR quadtree and R-tree polygonization algorithms, the merging and updating process continues up the entire R^+-tree until all lines are contained in a single node and all necessary broadcasts have been made. The execution time is analyzed in the same manner as that for the bucket PMR quadtree since the R^+-tree also makes use of a disjoint decomposition. However, the merging process is considerably more complex as we need to determine which

of the nodes being merged are adjacent so that we can perform the necessary update broadcasts.

8. Performance study

Experiments were conducted on a Thinking Machines CM-5 with 32 RISC processors and a total of 1 GB of RAM which implies 32 MB per processor. Fig. 20 displays the execution times for map polygonization for each of the three spatial data structures using the Prince Georges County map shown in Fig. 19. The Prince Georges County map contains approximately 35,000 line segments. Due to the per-

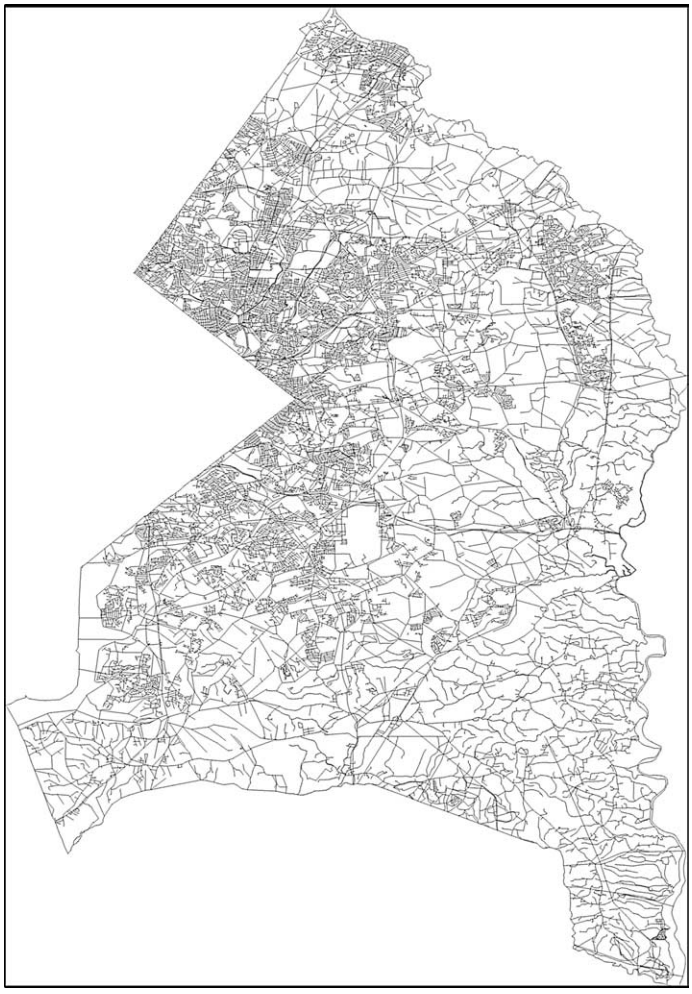

Fig. 19. Map of Prince Georges County, Maryland.

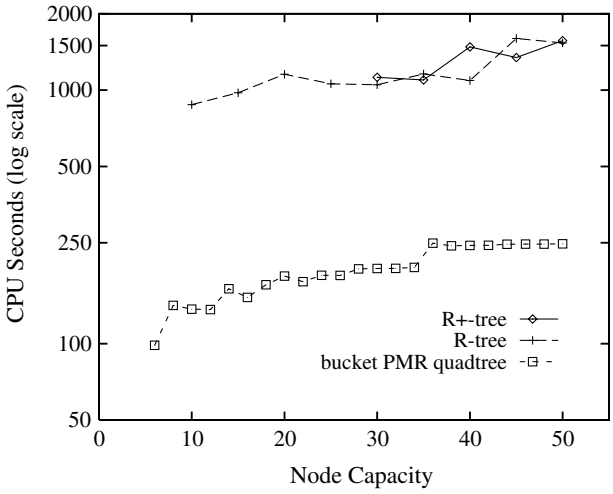

Fig. 20. Polygonization times for the three structures.

formance inefficiencies of the R^+-tree, a minimal occupancy level of 49.5% was employed, while the R-tree used the thirty percent level. From the figure it is clear that the bucket PMR quadtree offers significant performance advantages over both the R-tree and the R^+-tree. The difference is roughly one order of magnitude. It is attributed primarily to the considerable amount of time that the R-tree and the R^+-tree must spend in determining which nodes are intersecting (or adjoining in the case of the R^+-tree) when merging sibling nodes. For the bucket PMR quadtree, this computation is immediate as a result of regular decomposition. In addition, at each stage of the polygonization process, the R-tree and R^+-tree merge many more nodes/lines together; a node occupancy of n implies a fan-out of n. Alternatively, with the bucket PMR quadtree, four nodes are merged together at each stage of the computation. Essentially, the bucket PMR quadtree performs a larger number (equal to the height of the tree) of smaller node merges (with respect to the number of nodes being merged) than the R-tree and the R^+-tree.

The fact that the CPU time of the algorithms increases with node capacity, although slowly, is a result of the need to broadcast the endpoints of each line segment to all other lines in the node. As we pointed out in Section 5, this process is bounded by the maximal number of lines in a node. Clearly, modifying the node capacity does not necessarily prevent a decomposition from taking place which is why the execution time does not necessarily increase with every incremental increase in node capacity. This is especially true in light of the limited number of data sets that we used.

9. Concluding remarks

Data-parallel algorithms were presented for polygonizing a collection of line segments represented by a data-parallel bucket PMR quadtree, a data-parallel R-tree,

and a data-parallel R^+-tree. A sample performance comparison of the three data-parallel structures showed the data-parallel bucket PMR quadtree to be superior. Our performance comparison focussed on varying the data structure configurations (splitting thresholds, node capacities, search radii for range queries, etc.) rather than on the dataset sizes or the number of processors. Scalability and speedup are directions for future research, as is the implementation of other operations such as spatial join which is a special case of the join operation [9] where the join condition usually involves coverage of the same part of space. The spatial join is of interest because it involves more than one dataset and its performance depends on how well the data structure can correlate the areas of interest on the different datasets.

References

[1] B.G. Baumgart, Winged-edge polyhedron representation, Artificial Intelligence Laboratory AIM-179, Stanford University, Stanford, CA, October 1972.
[2] N. Beckmann, H.-P. Kriegel, R. Schneider, B. Seeger, The R*-tree: an efficient and robust access method for points and rectangles, in: Proceedings of the 1990 ACM SIGMOD International Conference on Management of Data, Atlantic City, NJ, May 1990, pp. 322–331.
[3] T. Bestul, Parallel Paradigms and Practices for Spatial Data, Ph.D. Thesis, University of Maryland, College Park, MD, April 1992, also University of Maryland Computer Science Technical Report CS–TR–2897.
[4] G.E. Blelloch, Scans as primitive parallel operations, IEEE Transactions on Computers 38 (11) (1989) 1526–1538, also Proceedings of the 1987 International Conference on Parallel Processing, St Charles, IL, August 1987.
[5] G.E. Blelloch, Vector Models for Data-Parallel Computing, MIT Press, Cambridge, MA, 1990.
[6] G.E. Blelloch, J.J. Little, Parallel solutions to geometric problems on the scan model of computation, in: D.H. Bailey (Ed.), Proceedings of the 1988 International Conference on Parallel Processing, vol. 3, St Charles, IL, August 1988, pp. 218–222.
[7] D. Comer, The ubiquitous B-tree, ACM Computing Surveys 11 (2) (1979) 121–137.
[8] D. Culler, R. Karp, D. Patterson, A. Sahay, K.E. Schauser, E. Santos, R. Subramonian, T. von Eicken, Log *P*: towards a realistic model of parallel computation, in: Proceedings of the Fourth ACM SIGPLAN Symposium on Principles and Practice of Parallel Programming, San Diego, May 1993, pp. 1–12.
[9] R. Elmasri, S.B. Navathe, Fundamentals of Database Systems, third ed., Addison-Wesley, Reading, MA, 2000.
[10] W.R. Franklin, Adaptive grids for geometric operations, Cartographica 21 (2–3) (1984) 160–167.
[11] M. Freeston, A general solution of the *n*-dimensional B-tree problem, in: Proceedings of the ACM SIGMOD International Conference on Management of Data, San Jose, CA, May 1995, pp. 80–91.
[12] M.W. Freeston, The BANG file: a new kind of grid file, in: Proceedings of the 1987 ACM SIGMOD International Conference on Management of Data, San Francisco, May 1987, pp. 287–300.
[13] O. Günther, Efficient structures for geometric data management, Ph.D. Thesis, University of California, Berkeley, CA, 1987, Lecture Notes in Computer Science 337, Springer-Verlag, Berlin, 1988.
[14] R.H. Güting, D. Papadias, F.H. Lochovsky (Eds.), Advances in Spatial Databases—Sixth International Symposium, SSD'99, Hong Kong, July 1999, also Springer-Verlag Lecture Notes in Computer Science 1651.
[15] A. Guttman, R-trees: a dynamic index structure for spatial searching, in: Proceedings of the 1984 ACM SIGMOD International Conference on Management of Data, Boston, June 1984, pp. 47–57.

[16] A. Henrich, H.W. Six, P. Widmayer, The LSD tree: spatial access to multidimensional point and non-point data, in: P.M.G. Apers, G. Wiederhold (Eds.), Proceedings of the Fifteenth International Conference on Very Large Data Bases, Amsterdam, August 1989, pp. 45–53.
[17] J. JáJá, P.Y. Wang, Special issue on data parallel algorithms and programming: guest editors' introduction, Journal of Parallel and Distributed Computing 21 (1) (1994) 1–3.
[18] I. Kamel, C. Faloutsos, Parallel R-trees, in: Proceedings of the 1992 ACM SIGMOD International Conference on Management of Data, San Diego, June 1992, pp. 195–204.
[19] M. Lindenbaum, H. Samet, A probabilistic analysis of tree-based sorting of large collections of line segments, Computer Science Department CS-TR-3455, University of Maryland, College Park, MD, April 1995.
[20] D. Nassimi, S. Sahni, Data broadcasting in SIMD computers, IEEE Transactions on Computers C 30 (2) (1981) 101–107.
[21] R.C. Nelson, H. Samet, A consistent hierarchical representation for vector data, Computer Graphics 20 (4) (1986) 197–206, also Proceedings of the SIGGRAPH'86 Conference, Dallas, August 1986.
[22] R.C. Nelson, H. Samet, A population analysis for hierarchical data structures, in: Proceedings of the 1987 ACM SIGMOD International Conference on Management of Data, San Francisco, May 1987, pp. 270–277.
[23] J. Nievergelt, H. Hinterberger, K.C. Sevcik, The grid file: an adaptable symmetric multikey file structure, ACM Transactions on Database Systems 9 (1) (1984) 38–71.
[24] G. Peano, Sur une courbe qui remplit toute une aire plaine, Mathematische Annalen 36 (1890) 157–160.
[25] J.T. Robinson. The k-d-B-tree: a search structure for large multidimensional dynamic indexes, in: Proceedings of the 1981 ACM SIGMOD International Conference on Management of Data, Ann Arbor, MI, April 1981, pp. 10–18.
[26] H. Samet, Applications of Spatial Data Structures: Computer Graphics, Image Processing, and GIS, Addison-Wesley, Reading, MA, 1990.
[27] H. Samet, The Design and Analysis of Spatial Data Structures, Addison-Wesley, Reading, MA, 1990.
[28] H. Samet, R.E. Webber, Storing a collection of polygons using quadtrees, ACM Transactions on Graphics 4 (3) (1985) 182–222, also Proceedings of Computer Vision and Pattern Recognition 83, Washington DC, June 1983, pp. 127–132, and University of Maryland Computer Science Technical Report CS–TR–1372.
[29] M. Scholl, A. Voisard (Eds.), Advances in Spatial Databases—Fifth International Symposium, SSD'97, Berlin, Germany, July 1997, also Springer-Verlag Lecture Notes in Computer Science 1262.
[30] J.T. Schwartz, Ultracomputers, ACM Transactions on Programming Languages and Systems 2 (4) (1980) 484–521.
[31] B. Seeger, H.-P. Kriegel. The Buddy-tree: an efficient and robust access method for spatial data base systems, in: D. McLeod, R. Sacks-Davis, H. Schek (Eds.), Proceedings of the Sixteenth International Conference on Very Large Data Bases, Brisbane, Australia, August 1990, pp. 590–601.
[32] T. Sellis, N. Roussopoulos, C. Faloutsos, The R^+-tree: a dynamic index for multi-dimensional objects, in: P.M. Stocker, W. Kent, P. Hammersley (Eds.), Proceedings of the Thirteenth International Conference on Very Large Data Bases, Brighton, England, September 1987, pp. 507–518, also University of Maryland Computer Science Technical Report CS–TR–1795.
[33] W. Wang, J. Yang, R. Muntz, PK-tree: a spatial index structure for high dimensional point data, in: K. Tanaka, S. Ghandeharizadeh (Eds.), Proceedings of the Fifth International Conference on Foundations of Data Organization and Algorithms (FODO), Kobe, Japan, November 1998, pp. 27–36.